

# Patterned vegetation, tipping points, and the rate of climate change

Theodore Kolokolnikov

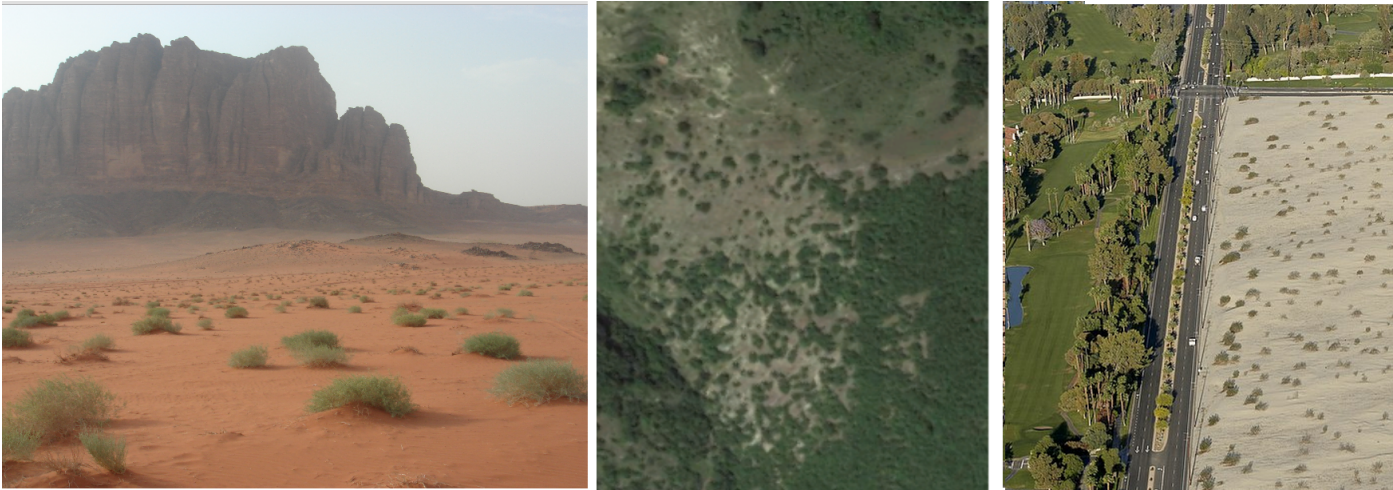
Joint work with Yuxin Chen, Justin Tzou and Chunyi Gai

June 9, 2015

# Introduction

- Climate change – both anthropogenic and natural – poses multiple pressures on earth ecosystems.
- While the earth's climate has undergone many drastic changes in its history, the rate at which the current human-induced changes are occurring is unmatched in recent history going back at least 60 million years.
  - The rate of CO<sub>2</sub> increase is more than 200 times the fastest historical rates of at least the last 800,000 years, as measured by ice cores
  - Ocean acidification is another indicator with unparalleled change in earth's known history.
- Large swings in earth's climate are not unprecedented, and life has been able to adapt to such swings more or less successfully in the past. The question is whether a species is resilient enough not just to the *changes* in environment, but to the *speed* with which these changes occur.
- The speed of climate change is especially important for an ecosystem that is already under stress, such as vegetation in arid and semi-arid environments, where a relatively small change in precipitation can have a very large impact.

# Vegetation patterns



- Vegetation adapts to arid environments by growing in patches, where it can conserve water
- Many mathematical models have been proposed, one of the best-known is Klausmeier Model (1999)

# Klausmeier model

A reaction-diffusion PDE:

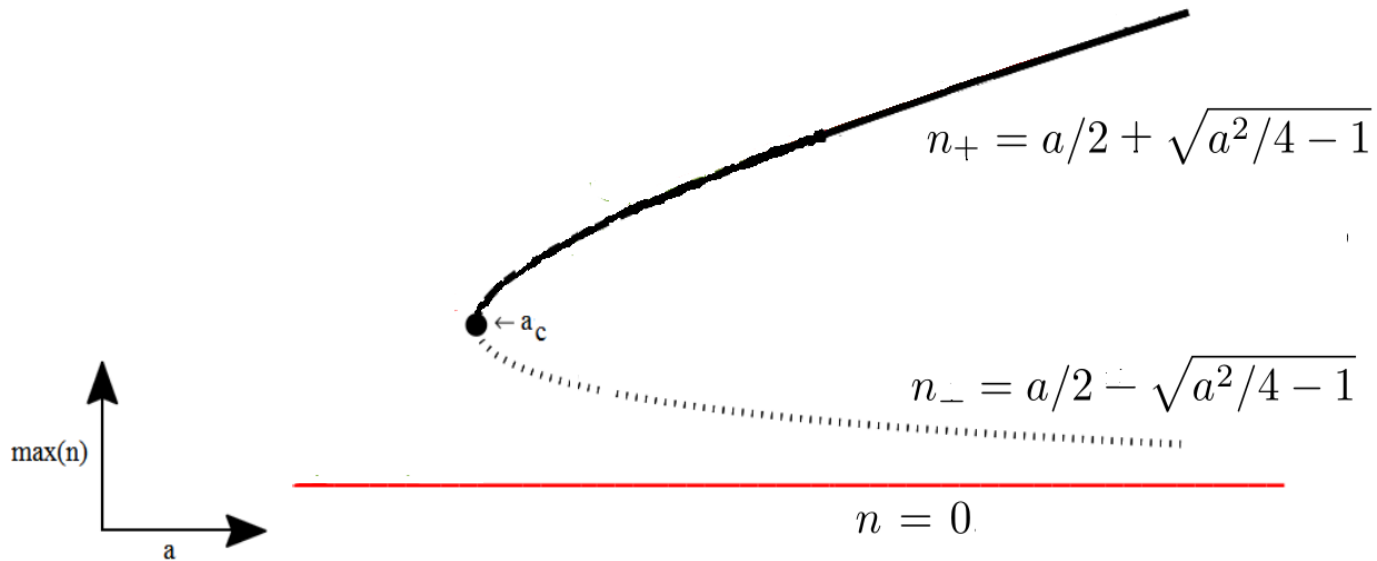
- $w(x, t)$  : water concentration
- $n(x, t)$  : plant density

$$\underbrace{\frac{\partial n}{\partial t}}_{\text{rate of plants}} = \underbrace{wn^2}_{\text{water intake}} - \underbrace{n}_{\text{plant death}} + \delta \underbrace{\frac{\partial^2 n}{\partial x^2}}_{\text{plant spread}},$$

$$\underbrace{b \frac{\partial w}{\partial t}}_{\text{rate of water}} = \underbrace{a}_{\text{precipitation}} - \underbrace{w}_{\text{evaporation}} - \underbrace{wn^2}_{\text{plant intake}} + \underbrace{c \frac{\partial w}{\partial x}}_{\text{flow (downhill)}} + \underbrace{d \frac{\partial^2 w}{\partial x^2}}_{\text{diffusion (through soil)}}.$$

# Classical “tipping point” theory: ODE

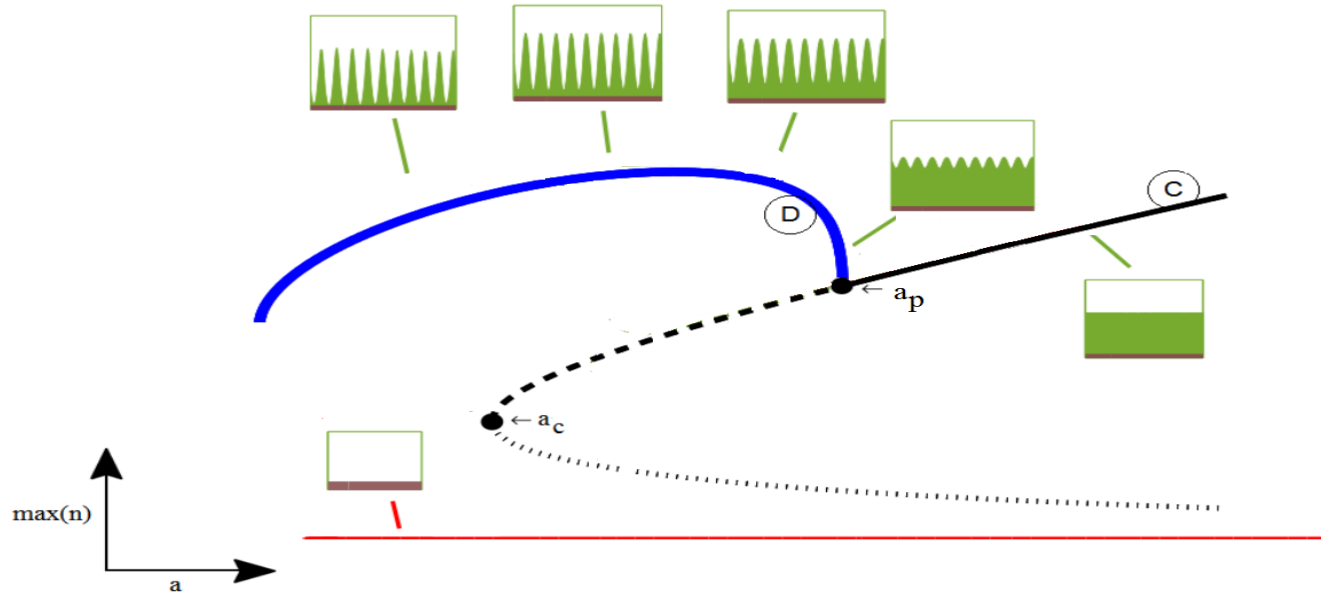
$$\frac{dn}{dt} = \delta \frac{d^2 n}{dx^2} - n + wn^2, \quad b \frac{dw}{dt} = a - w - wn^2$$



# Effect of diffusion

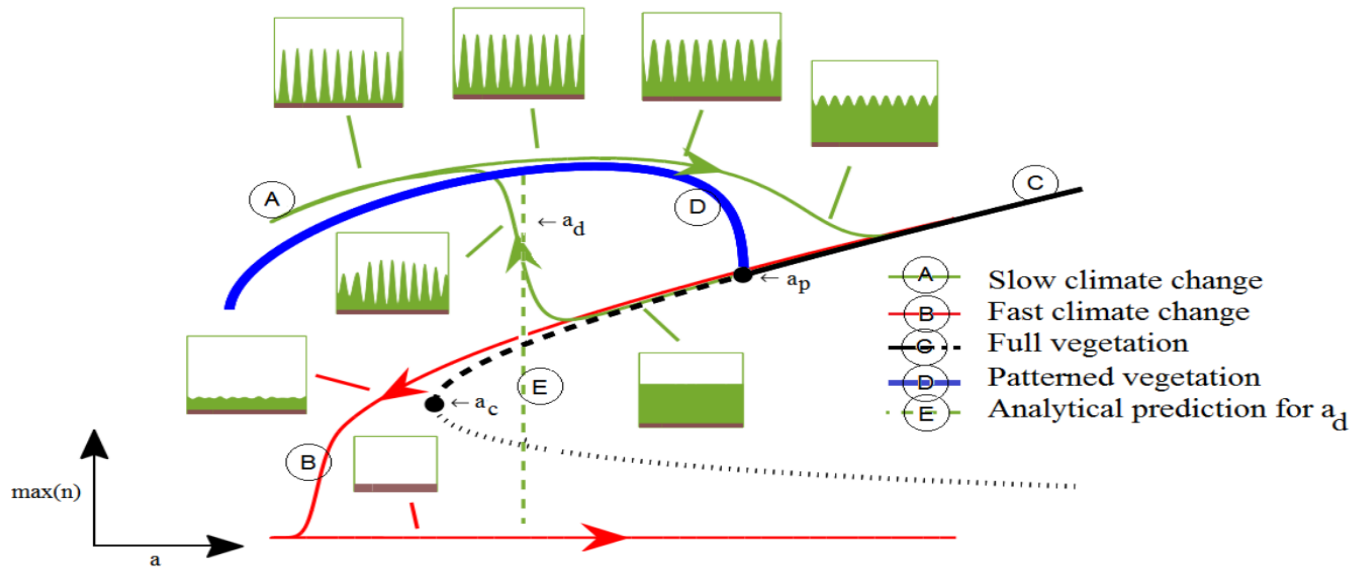
- Simplify: take  $b = 0, c = 0, \delta = 0.05$  :

$$\frac{dn}{dt} = \delta \frac{d^2n}{dx^2} - n + wn^2, \quad 0 = \frac{d^2w}{dx^2} + a - w - wn^2$$



- Turing bifurcation at  $a = a_p = 2.5$ ; fold-point (tipping-point) bifurcation at  $a = a_c = 2$ .
- Transition from full vegetation state to patterned vegetation as the precipitation  $a$  is decreased
- The patterned state survives for precipitation values  $a$  **below** the tipping point!

# What happens as $a$ is decreased slowly?



- $a = a_0 + (a_1 - a_0) (1 - \cos(\epsilon t)) / 2 + \text{small noise}$
- Extinction when  $\epsilon = 0.03$  ("fast precipitation change");
- Resilience when  $\epsilon = 0.006$  ("slow precipitation change")
- Depends on the level of noise too!
- Question: how do we quantify this?

# Analysis

$$\frac{dn}{dt} = \delta \frac{d^2 n}{dx^2} - n + wn^2, \quad 0 = \frac{d^2 w}{dx^2} + a - w - wn^2$$

$$a = a_0 - \varepsilon t + \sigma_0 \frac{dW}{dt}; \quad \varepsilon \ll 1, \sigma_0 \ll 1; \quad (1)$$

$$dW = \sqrt{dt} \sum_{m=-\infty}^{\infty} \xi_m(t) \exp(imx); \quad \xi_m \equiv \text{gaussian random variable} \quad (2)$$

Linearize around the “full vegetation state”  $n_+ = a/2 + \sqrt{a^2/4 - 1}$ ,  $w_+ = 1/n_+$  :

$$n(x, t) = n_+(\varepsilon t) + \phi(x, t), \quad w(x, t) = w_+(\varepsilon t) + \psi(x, t),$$

so that

$$\frac{d\phi}{dt} + \varepsilon n'_+(\varepsilon t) = \delta \frac{d^2 \phi}{dx^2} + \phi + n_+^2 \psi, \quad (3)$$

$$0 = \left[ \frac{d^2 \psi}{dx^2} + (-1 - n_+^2) \psi - 2\phi \right] dt + \sigma_0 dW. \quad (4)$$



Decompose in fourier modes:

$$\phi(x, t) = \sum \phi_m(t) e^{imx}, \quad \psi(x, t) = \sum \psi_m(t) e^{imx},$$

$$\frac{d\phi}{dt} = -m^2\delta\phi + \phi + n_+^2\psi, \quad (5)$$

$$0 = [-m^2\psi + (-1 - n_+^2)\psi - 2\phi] dt + \sigma_0\sqrt{dt}\xi. \quad (6)$$

Eliminate  $\psi$  :

$$d\phi = \alpha(\varepsilon t)\phi dt + \beta(\varepsilon t)\sqrt{dt}\xi, \quad (7)$$

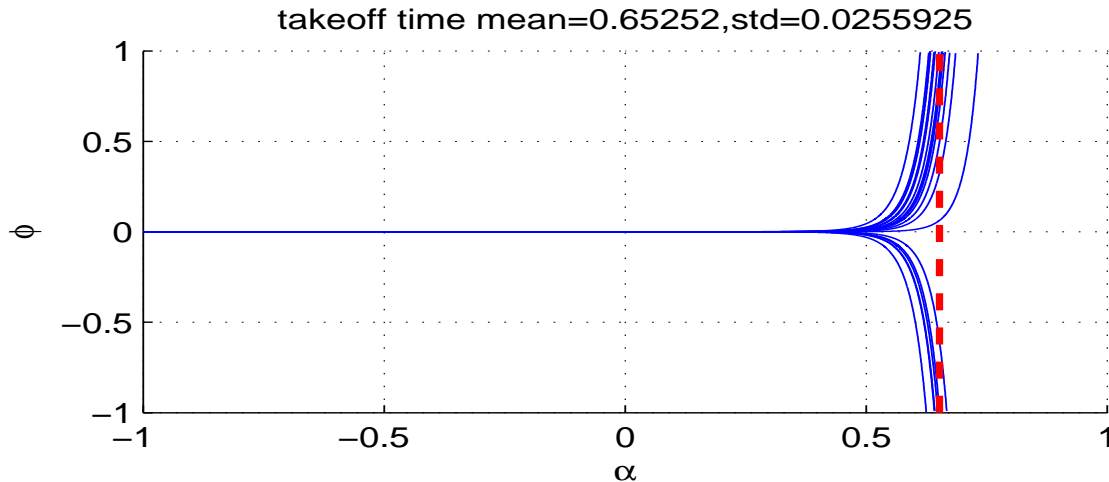
where  $\xi$  is a Gaussian random variable with mean zero and variance 1 and where

$$\alpha(s) = -m^2\delta + 1 - \frac{2n_+^2(s)}{m^2 + 1 + n_+^2(s)}, \quad \beta(s) = \frac{\sigma_0 n_+^2(s)}{m^2 + 1 + n_+^2(s)}, \quad s = \varepsilon t \quad (8)$$

Equation (7) is a variant of an Ornstein–Uhlenbeck process, with coefficients that are slowly changing in time.

**Example:**  $d\phi = \alpha(\varepsilon t)\phi dt + \beta(\varepsilon t)\sqrt{dt}\xi$ ,  $\phi(0) = 0$ .

- Take:  $\alpha(s) = -1 + s$ ,  $\varepsilon = 0.02$ ,  $\beta = 10^{-5}$ .



- The zero state becomes “unstable” at  $s_p = 1$ ,  $\alpha = 0$ . However the bifurcation is “delayed” and  $\phi$  “blows up” at a much later time, around  $\alpha = \alpha_d = 0.65$  here.
- Numerically, we define the “delayed time” to be when  $|\phi|$  crosses 1.
- There are 20 realizations plotted, the delayed time appears to be roughly the same! So we can define the “delayed time” in a consistent way.

- Below, we will show that

$$\alpha_d = \sqrt{-2\varepsilon \ln \left\{ \beta \left( \frac{\pi}{\varepsilon} \right)^{1/4} \right\}}$$

If  $\varepsilon = 0.02$  and  $\beta = 10^{-5}$  then  $\alpha_d \approx 0.64$ , excellent agreement with the simulations!

## Analysis of $d\phi = \alpha(\varepsilon t) \phi dt + \beta(\varepsilon t) \sqrt{dt} \xi$ , $\phi(0) = 0$ .

The density satisfies the Fokker-Planck PDE given by

$$\varepsilon \frac{\partial}{\partial s} u + \alpha(s) \frac{\partial}{\partial \phi} (\phi u) = \frac{\beta^2(s)}{2} \frac{\partial^2 u}{\partial \phi^2}, \quad u(\phi, 0) = \delta(\phi). \quad (9)$$

The exact solution is

$$u(\phi, s) = \frac{1}{\sqrt{2\pi\sigma}} \exp\left(-\frac{x^2}{2\sigma^2}\right);$$

$$\sigma^2(s; m) = \int_0^s \beta^2(\tau) \exp\left(-\frac{2}{\varepsilon} \int_\tau^s \alpha(\rho) d\rho\right) d\tau. \quad (10)$$

Let  $s_p$  be the such that that  $\alpha(s_p) = 0$ , and we assume that  $\alpha'(s_p) > 0$ . That is,  $s_p$  is the point at which the mode  $m$  becomes unstable. Then for  $s > s_p$ , Laplace's method yields

$$\sigma(s; m) \sim \exp\left(\frac{1}{\varepsilon} \int_{s_p}^s \alpha(\tau) d\tau\right) \beta(s_p) \left(\frac{\pi}{\varepsilon \alpha'(s_p)}\right)^{1/4}, \quad (11)$$

We define the “take-off” time  $s_d = s_d(m)$  for the mode  $m$  to be such that  $\sigma(s_d; m) = 1$ . Alternatively,  $s_d$  is such that  $\sigma \ll 1$  when  $s < s_d$  and  $\sigma \gg 1$  when  $s > s_d$ . For a fixed mode  $m$ , the value of  $s_d$  is therefore found by solving simultaneously

$$\alpha(s_p) = 0; \quad (12)$$

$$\int_{s_p}^{s_d} \alpha(s) ds + \varepsilon \log \left( \beta(s_p) \left( \frac{\pi}{\varepsilon \alpha'(s_p)} \right)^{1/4} \right) = 0. \quad (13)$$

This yields the time  $s_d$  at which the solution density spread  $\sigma$  for a given mode  $m$  starts to grow exponentially fast.

- Similar results – for SDE's – were derived using a related approaches in [Kuske, 1999] and [Berglund & Gentz, 2002].

## Back to Klausmeier model:

- The first mode that gets activated yields the delayed take-off value for

$$a_d \equiv a(\min_m s_d(m); m), \quad (14)$$

Note that, depending on the parameters, a solution for  $s_d$  may not exist, in which case the corresponding mode  $m$  is never activated. If  $s_d$  does not exist for any mode, the patterned state is never activated resulting in extinction.

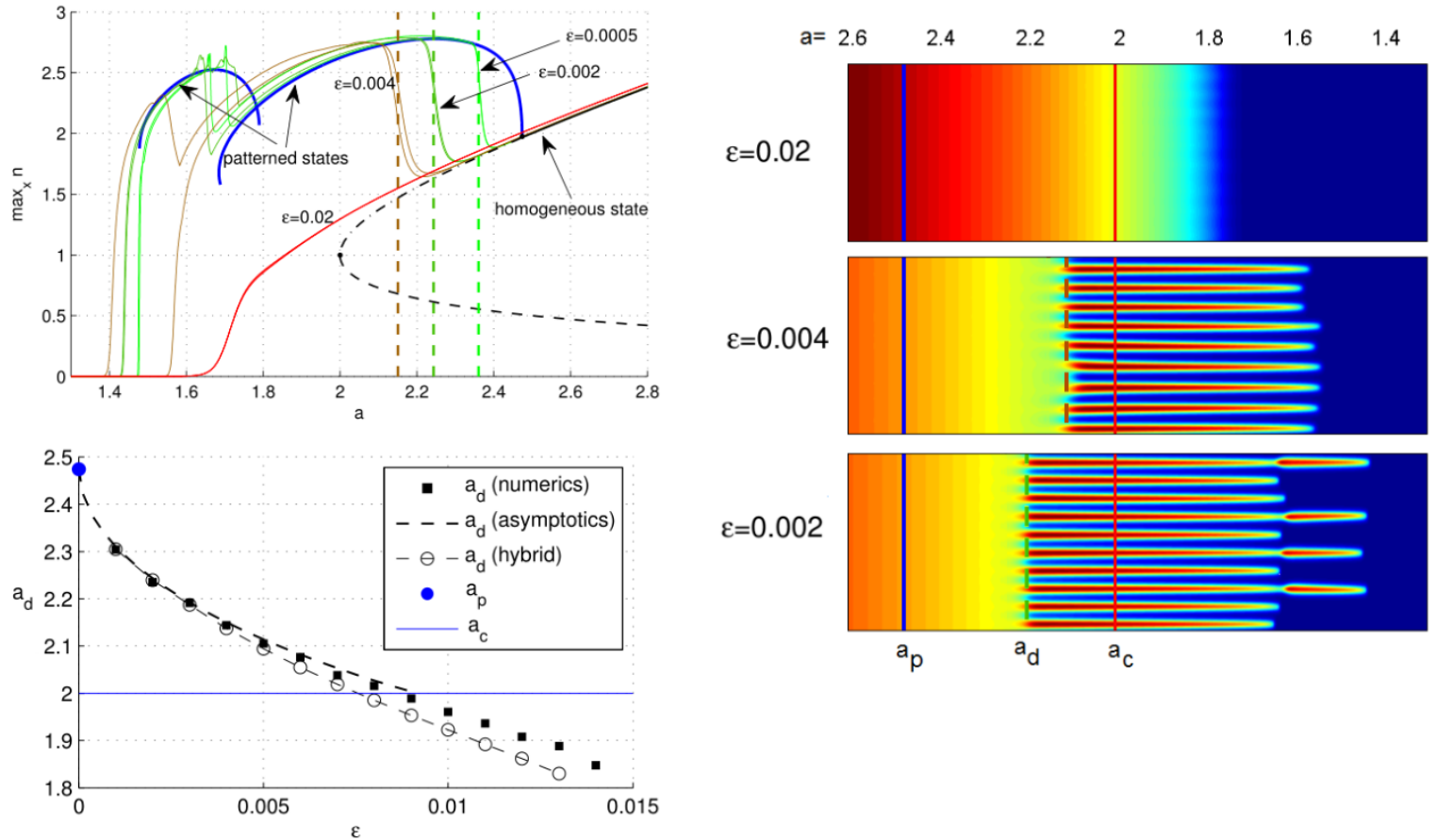


FIG. 2. Numerical verification of  $a_d$  as given in (16) for (6). The slow drift is taken to be  $a = a_0 - \epsilon t$  with  $a_0 = 3$ ,  $\sigma_0 = 0.0001$ ,  $L = 22.839$  and  $\delta = 0.05$ . Top left: the evolution of  $\max_x n$  as a function of  $a$  with  $\epsilon$  as indicated. The dashed lines show  $a_d$  as given by (16). The patterned state (blue on-line) to the left corresponds to a single-bump solution, whereas the patterned state on the right corresponds to the wave-number 10 born from a Turing bifurcation at  $a = a_p = 2.47439$ . Top right: color plot of  $n(x, t)$  as it evolves in time. The Turing bifurcation point  $a_p$ , the delayed bifurcation  $a_d$  and the fold point  $a_c = 2$  are indicated. Bottom left: Comparison of asymptotic and full numerical results for  $a_d$ . The hybrid curve is obtained by using the full homogeneous state (17) instead of (7) when computing (16). The value of  $a_d$  is estimated numerically as discussed in the text, and an average over 50 simulations is used. We used  $N = 100$ ,  $dt = 0.1$  (see Appendix A for numerical implementation details).

# Conclusions

- We have used a simple mathematical model to illustrate how patterned states can provide a refuge and prevent extinction under stressed conditions, even as the precipitation falls below the tipping point of a homogeneous state.
- Under slow climate change, the patterned state can recover to the full vegetation state when precipitation is dialed back to favorable conditions.
- If precipitation decreases too quickly past the tipping point, the system may have no time to transition to the patterned state before the tipping point is reached, resulting in an irreversible extinction.
- This simple mechanism underscores the key role that spatial heterogeneity and noise have on the resilience of the system. It also illustrates the importance of not only the absolute level of climate change, but also the *speed* with which it occurs.
- Reference:
  - Yuxin Chen, Theodore Kolokolnikov, Justin Tzou and Chunyi Gai, "Patterned vegetation, tipping points, and the rate of climate change", to appear, European Journal of Applied Math.



